Development of a Transient Simulation Program for Micro Gas Turbines and its Application to a 30kW class engine

Min Jae Kim[a], Jeong Ho Kim[b] and Tong Seop Kim[c]

[a] Graduate School, Inha University, 402-751, Republic of Korea, 22142212@portal.inha.kr
[b] Graduate School, Inha University, 402-751, Republic of Korea, amour8040@naver.com
[c] Department of Mechanical Engineering, Inha University, 402-751, Republic of Korea, kts@inha.ac.kr

Abstract:

It is important to design a robust control system to secure reliable operation of gas turbines in a wide operating range. Using precise simulation software that predicts transient behaviour would remarkably reduce the time and effort to obtain a variety of running data by real engine test. In this research, an in-house program based on physical models was developed to simulate dynamic behaviour of micro gas turbines. Major components of a micro gas turbine are a compressor, a turbine, a combustor and a recuperative heat exchanger. A special attention was given to the modeling of the counter-flow recuperative heat exchanger between hot exhaust gas and compressor discharge air. The recuperator was divided into several segments and linearized modeling was used to shorten computing time while a high accuracy was guaranteed. Scaled performance maps of compressor and turbine was used to simulate a 30kW class commercial engine. An off-design model refinment procedure was adopted to overcome the lack of information of component characteristics. A unique method using transient operation data duing a normal shut-down was adopted to estimate the thermal capacity of the recuperator which is a critical parameter required for dynamic simulation. Dynamic operation due to stepwise power changes was simulated using control logic. Overall good agreement between simulation and real operation confirmed the validity of the developed program.

Keywords:

Control, Micro Gas Turbine, Simulation, Thermal Inertia, Transient Behaviour.

1. Introduction

Developing a new gas turbine engine takes much effort. One of the effective ways to reduce development time and cost is to have a reliable simulation program that can replace various engine tests. A good simulation program can be used for diverse purposes such as performance prediction, diagnosis and controller development. Actual physical phenomena in a gas turbine can be modeled precisely only by complex nonlinear mathematical equations. In the past, however, linearized equations were used due to technical limitations. These days, many limitations have been overcome by rapid development of computing capability and engine simulations using complex non-linear modeling are being tried. Prediction of transient behaviour during start-up, shut-down and load change is the most essential task of engine simulation and a prerequisite for development of a robust engine control system. Therefore, simulations based on physical models have been actively pursued recently. Some examples are modeling of load follow operation and start-up [1, 2], dynamic behaviour simulation for control system setup and test [3], and a comparison between physical and statistical methods [4]. Most of the studies have dealt with large gas turbines for central power stations.

Research and development of micro gas turbines (MGTs) have also been made actively during the past decades as the demand for distributed generation has grown rapidly. An MGT is a small gas turbine, less than several hundreds of kilowatts. Fig. 1 illustrates an example of MGT layout, which was used in this study. An MGT is a recuperated Brayton cycle thermodynamically. Simplicity is the major target of most MGT developments, leading to using a single stage centrifugal compressor and a single stage radial turbine without cooling. Such a choice inevitably requires a low turbine

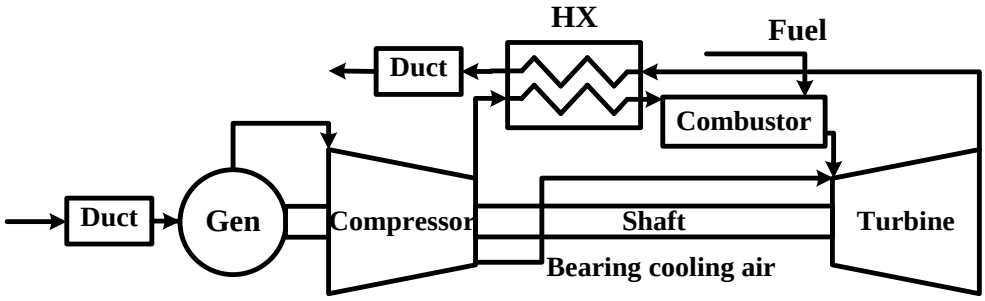

Fig. 1. Schematic configuration of a micro gas turbine

inlet temperature as well as a low pressure ratio, which leads to a very low thermal efficiency compared to large gas turbines. To overcome the low efficiency, a recuperator is installed. Efficiencies over 30% are available these days. Transient behaviour analysis is as important as in large gas turbines because an MGT usually suffers frequent start-up, load change and shut-down. Accordingly, several dynamic simulation studies on MGTs have been performed recently. Some examples are transient behaviour analysis and control of MGT based cycles [5], comparison between simulation and test [6] and influence of recuperator volume on surge margin [7].

The ultimate goal of our research is to develop a reliable dynamic analysis program which can be used as a simulator for engine development. This paper presents the first step of our research and covers program setup and validation using a commercial engine. A unique feature of this study is that we figured out several critical component parameters of the engine such as thermal inertia and heat transfer characteristic parameter of the recuperator, which are unknown but important for dynamic simulation, by using both the steady state and dynamic analyses. After setting up dynamic modeling and control logic, transient behaviour due to load change was simulated and results were compared with actual operating data, providing program verifications.

2. Modeling and analysis

2.1. Outline

Fig. 2 describes the outline of the program development sequence. Mathematical modeling of every component and overall system and a subsequent steady-state design point simulation was the first step. The next step was modeling of off-design operational characteristics of all components (compressor, turbine, recuperator) and their refinement (i.e. tuning of model parameters) to match the simulated off-design operation data to steady-state test data. Then, the thermal inertia of the recuperator was determined using dynamic test data, especially during shut-down. Lastly, the dynamic simulation routine was completed by applying control logic and simulation for transient operation during load changes was performed.

2.2. Mathematical modeling

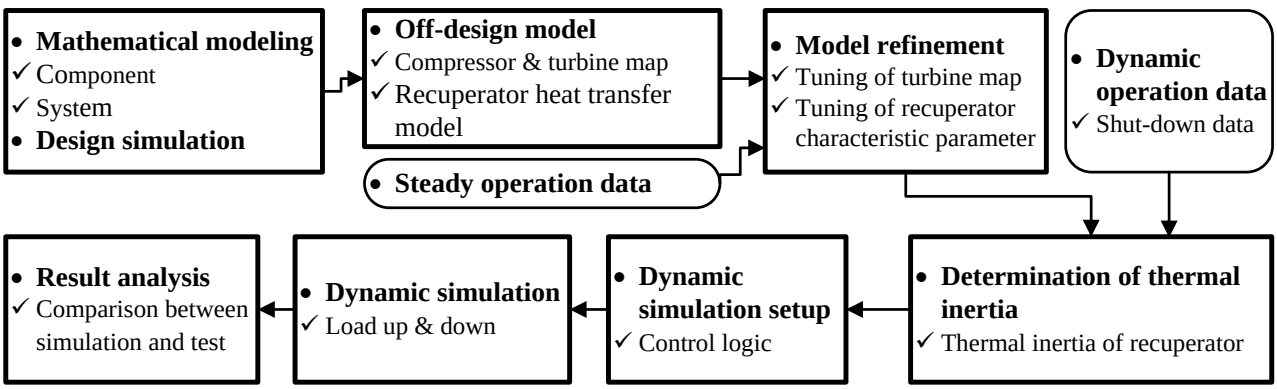

Fig. 2. Flow chart of program development and simulation

The MGT simulated in this study is C30 of Capstone Turbine Corporation which is installed in the present authors' laboratory. Major components are a core part (a centrifugal compressor, a combustor, a radial turbine and a recuperator), an air cooled high-speed generator and a digital power controller. Our simulation is limited to the operation of the core part. The MATLAB [8] was the programming framework, and object oriented programming was used to modularize each component. The advantages of object oriented programming are easy maintenance and multi-purpose use of the program.

Governing equations of each component are mass balance and energy conservation equations. All working fluids including the combustion gas were modeled as ideal gas mixtures and temperature dependent specific heat data [9] were integrated to obtain the enthalpy data in the energy equations. Isentropic efficiencies of the compressor and turbine were given in the design calculation and corrected in off-design and dynamic operations according to performance maps. Complete combustion of natural gas fuel was assumed. Pressure drops of all ducts and combustor were assigned in the design calculation and corrected in any other operation using a correction equation in [10]. In addition to the steady-state modeling mentioned above, dynamic modeling for the rotating part and the recuperator was needed. In all components, fluid inertia was neglected because the fluid flows sufficiently fast and volume of every component is small in a micro gas turbine. The torque balance of the rotating shaft connecting the turbine, the compressor and external load led to the following governing equation of the shaft, which determined the change in rotational speed of the shaft (the subscript *t* refers to the time). The external load (*L*) was given as input of the simulation. At each time step, compressor and turbine powers were calculated using quasi-steady assumptions neglecting fluid inertia. Then, a new shaft rotation speed at the next time step was predicted using the equation. The rotating inertia (*I*) and mechanical efficiency are constant.

$$\omega^{t+1} = \omega^{t} + \left(\Delta t / I\right)\omega^{t}\left(\dot{W}_T \eta_{me} - \dot{W}_C - L\right), \text{ where } \dot{W}_T = \dot{m}\left(h_{in} - h_{out}\right) \text{ and } \dot{W}_C = \dot{m}\left(h_{out} - h_{in}\right) \quad (1)$$

The recuperator is a counter-flow type heat exchanger and was modeled as a summation of many segments as conceptually drawn in Fig. 3. The energy equations of the recuperator are as follows.

$$\text{Cold side}: \dot{m}_c\left(h_{c,l} - h_{c,l-1}\right) = A\alpha_c\left[T_{HX,l-1} - \left(T_{c,l} + T_{c,l-1}\right)/2\right]$$

$$\text{Hot side}: \dot{m}_h\left(h_{h,l+1} - h_{h,l}\right) = A\alpha_h\left[\left(T_{h,l} + T_{h,l+1}\right)/2 - T_{HX,l}\right]$$

$$\text{Metal}: A\alpha_c\left[\left(T_{c,l} + T_{c,l+1}\right)/2 - T_{HX,l}\right] + A\alpha_h\left[\left(T_{h,l} + T_{h,l+1}\right)/2 - T_{HX,l}\right] = \left(mc\right)_{HX}\left[\left(T^{t}_{HX,l} - T^{t-1}_{HX,l}\right)/\Delta t\right] \quad (2)$$

The first two equations are integrated forms of a differential equation ($\dot{m}dh = dA\alpha\left(T_{HX} - T_{Flow}\right)$) and determine fluid temperatures. The third equation describes a transient energy balance of the heat exchanger metal and determines the metal temperature. An exact balance between the heat transfers from the hot side and to the cold side results in a steady-state. Using the enthalpies as they appear in these equations is desirable for a high calculation accuracy. However, it requires a time-consuming numerical technique such as the Newton-Raphson method to obtain converged solutions because the equation set is non-linear. Replacing the enthalpy change by $c_p \Delta T$ eliminates such a problem because temperatures directly appear as variables in the equations. Then, the equation set can be converted to a linear matrix, which is much easier to solve. The drawback of such a method is an

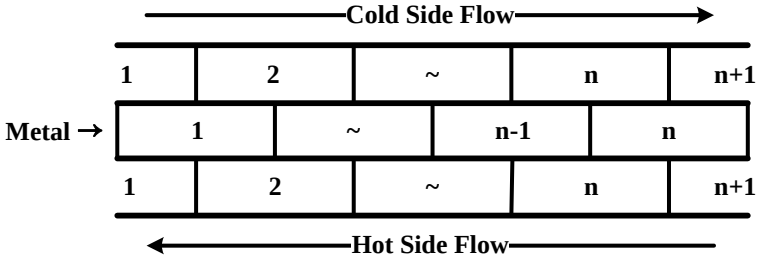

Fig. 3. Schematic diagram of a multi-segment counter-flow recuperator

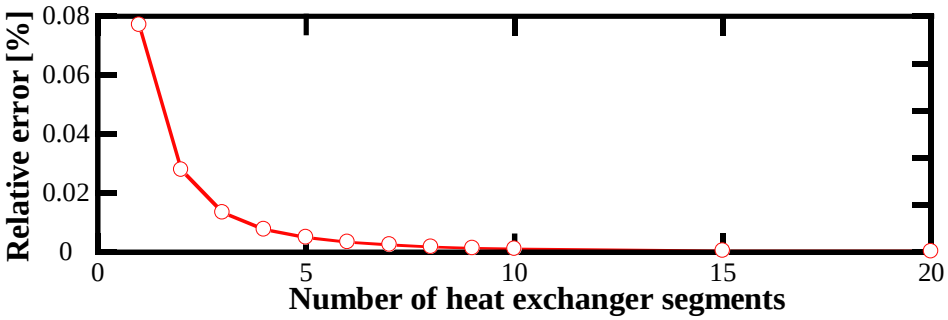

Fig. 4. Influence of number of segments on the heat balance error of the recuperator

inaccuracy in the energy balance accompanied by the assumption of constant specific heat. However, the inaccuracy naturally decreases in our modeling because we have to use multiple segments along the flow direction anyway. In such a circumstance, the c_p value of each segment depends on the fluid temperature in that segment, leading to a nearly continuously varying c_p along the flow direction. Accordingly, we adopted the linearlized calculation model in this study and checked the effect of number of segments in a steady-state condition at the design point. Fig. 4 shows the relative error in the energy balance between the hot and cold fluid sides. The error rapidly decreases as the number of segments increases, leading to less than 0.01% with more than four segments. We adopted seven segments in the simulations presented in this paper.

2.3. Design performance

The design simulation results are summarized in Table 1. Technical data needed for the design point calculation were referred to the manufacturer's reports [11,12]. The engine inlet air eliminates the heat release from the generator before flowing into the compressor. The air temperature rise was assumed to be 2.2ºC. Some of the compressor exit air cools the air bearing of the shaft and flows into the turbine. 1.5% of air extraction was assumed. Other miscellaneous losses such as pressure losses in the combustor, recuperator and ducts were also assigned. The calculated power output and thermal efficiency at the shaft end at ISO conditions (15ºC, 1 atm) were 36.1kW and 29.9%. The turbine exit temperature and the exhaust gas temperature after the recuperator were 593ºC and 277ºC.

2.4. Off-design modeling and refinement

To describe the operating characteristics of the compressor and turbine, performance maps were used. We had to use a scaled version of maps of small compressor and turbine in a database [13], specifications of which are similar to those of C30, because the actual maps of the engine were not available. Performance maps are usually drawn using semi-dimensionless speed and mass flow ($N/\sqrt{T_{in}}$, $M=\dot{m}\sqrt{T_{in}}/P_{in}$), pressure ratio and efficiency. The non-dimensional mass flow, efficiency and pressure ratio of the original maps were scaled according to the following rules [14]. The subscripts *d*, *m* and *s* mean design point, original map and scaled map.

$$M_s=\frac{M_d}{M_{m,d}}M_m,\ \eta_s=\frac{\eta_d}{\eta_{m,d}}\eta_m,\ PR_s=\frac{PR_d-1}{PR_{m,d}-1}\left(PR_m-1\right)+1 \tag{3}$$

Table 1. 30kW micro gas turbine design parameter

Component	Parameter	Value	Component	Parameter	Value
Compressor	Pressure Ratio	3.6	Recuperator	Gas outlet temperature	276.7 ºC
	Efficiency	79 %		Total pressure drop	3.8 %
Combustor	Heat loss	0.5 %	Turbine	Exit temperature	593.3 ºC
	Pressure drop	2 %		Efficiency	84 %
Shaft	Rotating speed	96000 RPM	Performance	Shaft power	36.1 kW
	Cooling Flow	1.5 %		Thermal efficiency	29.9 %

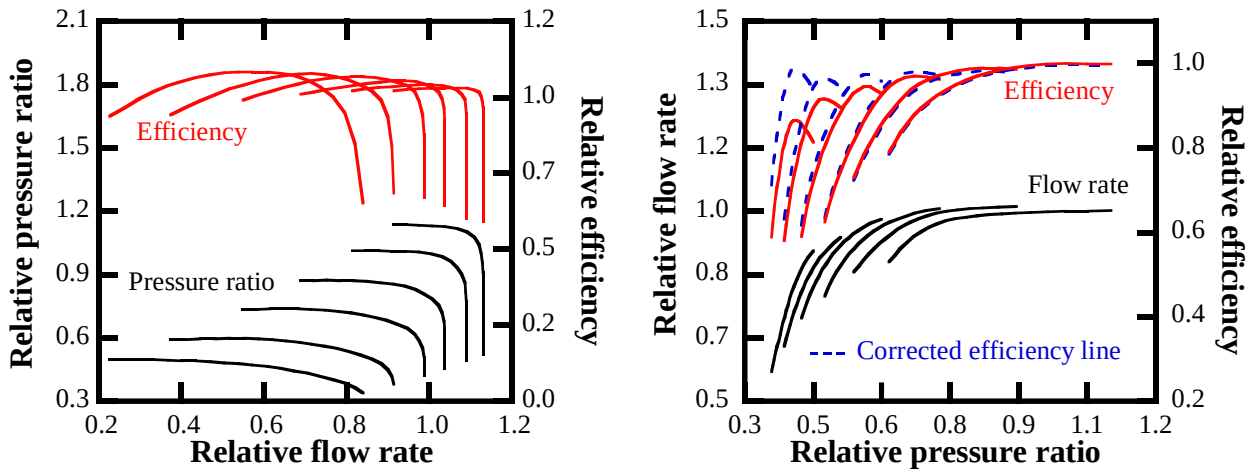

Fig. 5. Scaled performance maps of compressor and turbine: a) Compressor map, b) Turbine map

Fig. 5 shows the scaled compressor and turbine maps, where all of the parameters are represented by their relative values compared to design values. The dotted lines in the turbine map are refined efficiency curves. The details of the refinement procedure and results will be given later in this section and section 3.

The change in heat transfer coefficient governs the change of operating behaviour of the recuperator at off-design conditions. Heat transfer coefficient is affected by various flow properties but the major parameter is the fluid flow rate. Neglecting minor effects, the change in heat transfer coefficient can be described by the following equation.

$$\left(\dot{m}/\dot{m}_d\right)^i = \left(\alpha/\alpha_d\right) \tag{4}$$

The recuperator of C30 is a primary surface type compact heat exchanger and the value of index *i* was not known. But, according to literature [15, 16], the indices of similar compact heat exchangers are close to 0.8. Therefore, we used 0.8 as the reference value for the index and checked its validity in the model refinement step which is mentioned below.

After we set up the reference off-design models for the compressor, turbine and recuperator as mentioned above, we further refined the models using steady operation data. Fig. 6 describes variations of shaft power and operating parameters, such as turbine exit temperature and exhaust gas temperature and pressure, in terms of rotating speed, and covers the entire power range from a near zero shaft power to the full power. We also took the slight change of ambient condition (temperature, pressure and humidity) during the full range test into consideration for a higher accuracy of the refinement calculation. In addition to the parameters in Fig. 6, we also measured compressor discharge pressure to obtain pressure ratio. Except the turbine exit temperature which was measured by a temperature sensor embedded in the engine package, all of the other temperatures and pressures were measured by additionally installed K-type thermocouples and pressure transducers known to have accuracies of less than 0.75% and 0.1%, respectively. Fuel flow was measured by a volume flow meter. Its measuring accuracy is known to be better than 1% but the inaccuracy of mass flow rate in our system was thought to be higher than that because of the uncertainty in calculating the density of natural gas caused by the inaccuracy of its composition which could not be measured on site. Therefore, we did not use the measured fuel mass flow rate in the model refinement but compared it with calculated one as will be explained in section 3.

The target of off-design model refinement was to fine-tune the turbine efficiency of the turbine performance map and the heat transfer index *i* in (4). The refinement procedure is explained as follows. The compressor map of Fig. 5 was used without modification. Then, we performed steady-state off-design calculation with varying turbine efficiency and heat transfer index for each running point of Fig. 6 to make simulated power output, turbine exit temperature (TET) and exhaust gas temperature (EGT) as close as possible to measured data. In other words, we found out a set of three

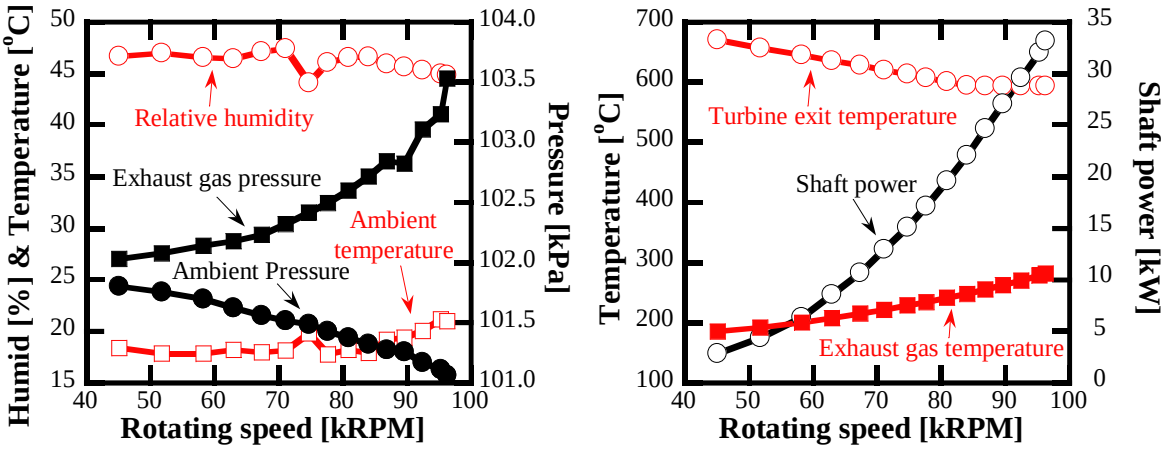

Fig. 6. Variations in measured operating parameters with shaft speed: a) Engine boundary conditions, b) Shaft power, turbine exit temperature and exhaust gas temperature

independent variables (fuel flow rate, turbine efficiency and heat transfer index) for each running point which best reproduced the three performance parameters (power, and two temperatures) as conceptually described by the following equation.

$$\left(\dot{W}_{sh}, TET, EGT\right) = f\left(\dot{m}_f, \eta_T, i\right) \tag{5}$$

2.5. Determination of thermal inertia

The thermal inertia of the recuperator plays an important role in dynamic response of recuperated cycle gas turbine [17]. It determines the time rag of the heat transfer from the hot gas to the cold air, which in turn affects all of the other parameters, especially temperatures. Therefore, knowing an exact value of the thermal capacity of the recuperator metal ($(mc)_{HX}$) in (2) is important. Of course, it is not available for the commercial engine we used. Hence, we worked out a way to estimate it using transient operation data. To eliminate effects of parameters other than thermal capacity, we needed uncontrolled operation where all of the internal parameters change naturally without any artificial manipulations. The normal shut-down procedure is appropriate for that purpose. Once the load is fully rejected and shut-down is commanded, fuel supply is stopped and the engine continues ideal operation with a fixed speed for some time. The air sucked into the engine cools down every component gradually until the turbine exit temperature reaches a target temperature. The main purpose of this procedure is to protect the engine from thermal shock caused by an abrupt shut-down. Thermal capacities of other components are much smaller than that of the recuperator. Therefore, it is quite feasible to assume that the variation in exhaust gas temperature with time is directly influences by the thermal capacity of the recuperator. Accordingly, we conducted dynamic shut-down simulation several times assuming various thermal capacity values of the recuperator, compared the simulated exhaust gas temperatures with those obtained from test and selected a optimal value.

2.6. Control logic

The most distinct feature of the micro gas turbine is that its shaft speed varies persistingly as power changes. A digital power controller coverts the variable frequency into a constant output frequency. The purpose of the variable speed operation is to maintain the turbine exit temperature as high as possible, which is beneficial to the partial load efficiency of recuperated cycle gas turbines [18]. Such a control is also adopted in C30 as shown in Fig. 6(b). In particular, turbine exit temperature is controlled to be almost constant in the operation range from 80 krpm which corresponds to about a half of full power to the full speed (96 krpm) producing full power. The control logic of the entire power range is not easy to simulate because we do not have sufficient information on the actual control of C30. Therefore, we limited our dynamic simulation only in the constant TET operation

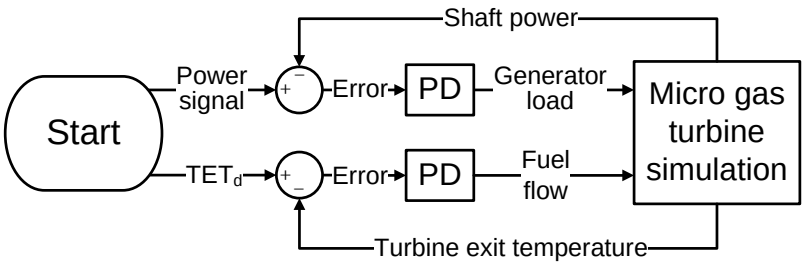

Fig. 7. PD Control logic

range. The control variables are turbine exit temperature and shaft power. Theoretically, the manipulated variables are fuel flow rate and rotating speed. However, we used the imbalance between power and load ($\dot{W}_T\eta_{me} - \dot{W}_C - L$) instead of rotating speed because the latter cannot be directly manipulated. A simple PD control logic [19] was used as in the following equations.

$$mv^{t+1} = mv^t + K_P\left\{e^t + K_D\left[\left(e^t - e^{t-1}\right)/\Delta t\right]\right\}, \text{ where } e = cv - cv_d \tag{6}$$

Control gains were found out by trial and error. Fig. 7 illustrates the concept of control logic.

3. Results and discussion

Fig. 8 shows the result of the off-design model refinement, the procedure of which was explained in the last paragraph of section 2.4. Fig. 8(a) presents the turbine efficiency and heat transfer index obtained from the refinement. Using the refined turbine efficiency, the original efficiency curve of the turbine map was corrected as shown by the dotted lines in Fig. 5(b). The heat transfer index remained at 0.8 in a high speed (and power) range, while it increases with speed reduction in a low speed range. A lower speed means a lower flow rate, and thus a lower Reynolds number. Application of our method in (4) to the graphical correlations in a database [20] resulted in increase of the index with decreasing Reynolds number, which confirms that the trend of Fig. 8(a) is feasible at least qualitatively. After finishing the model refinement, we performed the steady-state off-design analysis again using the corrected turbine map and index. The major simulation outputs (power, exhaust gas temperature, fuel flow rate, and compressor discharge pressure) were compared with measured test data and relative deviations are illustrated in Fig. 8(b). In the entire speed range (i.e. power range), the simulated exhaust gas temperature agreed very well with test data (maximum deviation is less than 1%). The agreement of turbine exit temperature was even better (not shown in the figure). The agreement of shaft power was also good: it should be noted that the 4% relative deviation in the lowest power (i.e. speed) point means only 0.1kW deviation in absolute power, which is only 0.3% of the full power. The deviation of the compressor discharge pressure (CDP) in

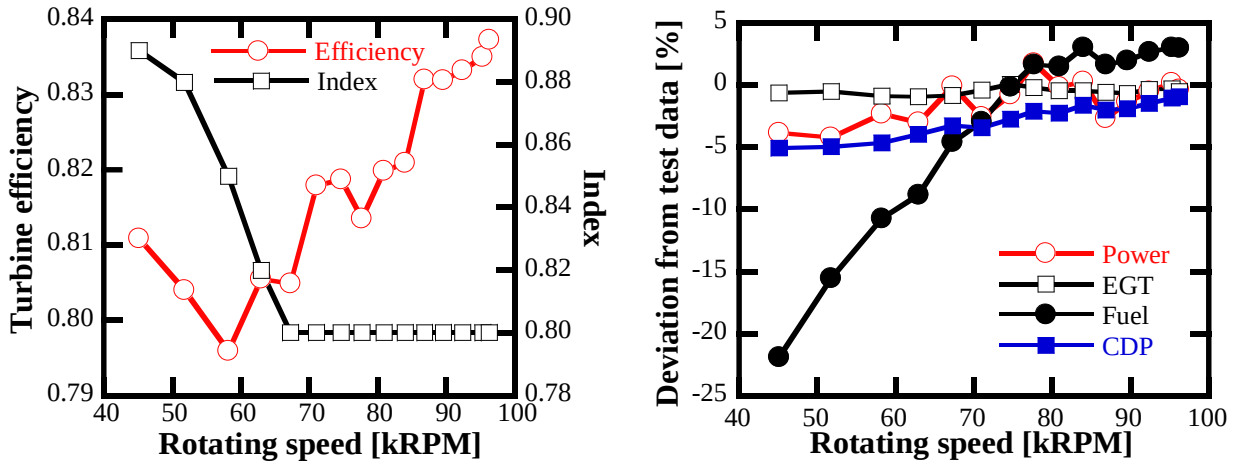

a) *b)*

Fig. 8. Result of off-design performance simulation: a) Refined turbine efficiency and heat transfer index, b) Deviation of simulated parameters from measured data.

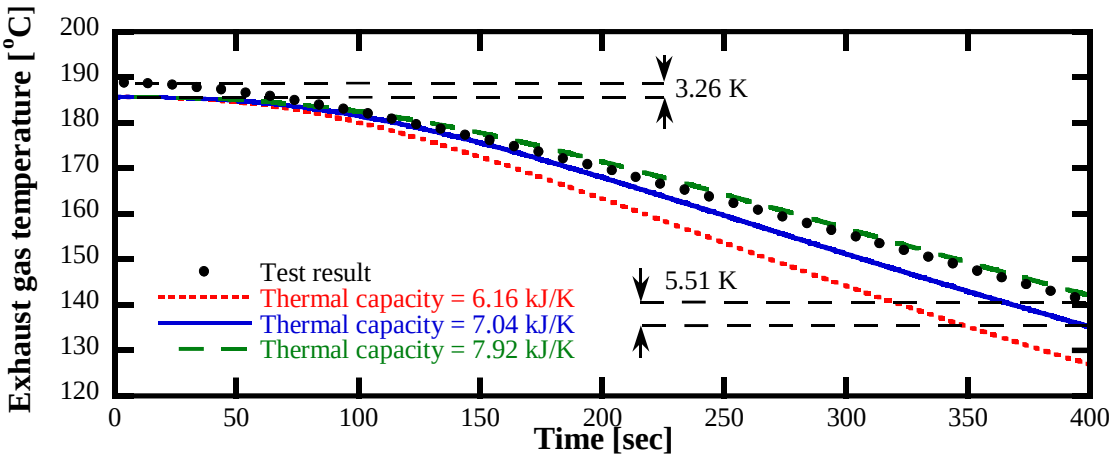

Fig. 9. Variation in exhaust gas temperature during a normal shut-down process

the high speed range is also tolerable. The increase in CDP with decreasing shaft speed is due to the limitation of the compressor map used in this study. It is not the actual map of the compressor of the engine we used but a map scaled from another one. Thus, the accuracy of the adopted map naturally decreases as the working point moves away from the design point, which is the main cause of the CDP deviation. The relatively large deviation of fuel flow rate is due to a couple of factors: uncertainty of fuel flow measurement and limitation of the used compressor map. The inaccuracy of the compressor map would cause incorrect air flow prediction, which in turn would distort the calculated fuel flow rate. The possibility of this happening is relatively large in the low speed range as explained above for the deviation of compressor discharge pressure. It is concluded that the scaled compressor map represents the actual compressor off-design behaviour reasonably in a high speed range (for example, over 80 krpm) but the deviation of the compressor characteristics of the map from actual ones becomes larger as the shaft speed (i.e. air flow) decreases. If we confine our interest to the range between 80 krpm and full speed for which our dynamic simulation was performed, the maximum deviation is less than 3%. Our ultimate research goal is to apply our program to the simulation of an engine to be developed. In such a case, the inaccuracy in the low speed range will be reduced sensibly because an exact compressor performance map will be provided by the engine manufacturer.

Fig. 9 shows a comparison of simulated and measured variations in the exhaust gas temperature during an entire shut-down period of 400 seconds. We varied the thermal capacity of the recuperator metal in the dynamic simulation as explained in section 2.5 to estimate a value which fitted the measured data best. 7.04 kJ/K was selected as the best fitting value considering the initial and final differences between the simulated and measured temperatures. Stainless steel or alloys such as SUS 347 and Inconel 625 are usually used for micro gas turbine recuperators [21]. The mass of the recuperator is presumed to be about 14 kg considering that the specific heats of those materials are about 0.5 kJ/kgK. The estimation of the recuperator mass using the database in the literature [21] is 16.8-23kg (recuperator effectiveness and a ratio between heat exchanger mass and fluid flow rate were used), which is close to our calculation.

After setting up the dynamic simulation program including the control logic, we simulated the dynamic behaviour of the engine in a high speed range where constant TET control was applied. Figs. 10 to 12 show the variations in major parameters. 1 to 2 kW stepwise power ups and downs were applied. All of the measured boundary conditions (ambient temperatures, pressures, relative humidity and exhaust pressure) were used in the simulation. The simulated results are compared with measured data in the figures and enlarged views are also provided. According to the results in the figures in the left hand side, the simulation follows the test trend very well macroscopically. The differences between simulation and test in the near-steady operation between two sudden power demands are due to the steady-state deviation as explained above regarding the results of Fig. 8. Once a sudden increase of power demand occurs, fuel and speed increase rapidly to satisfy the demand. Power generation also follows the demand as fast as the other two parameters. It should be

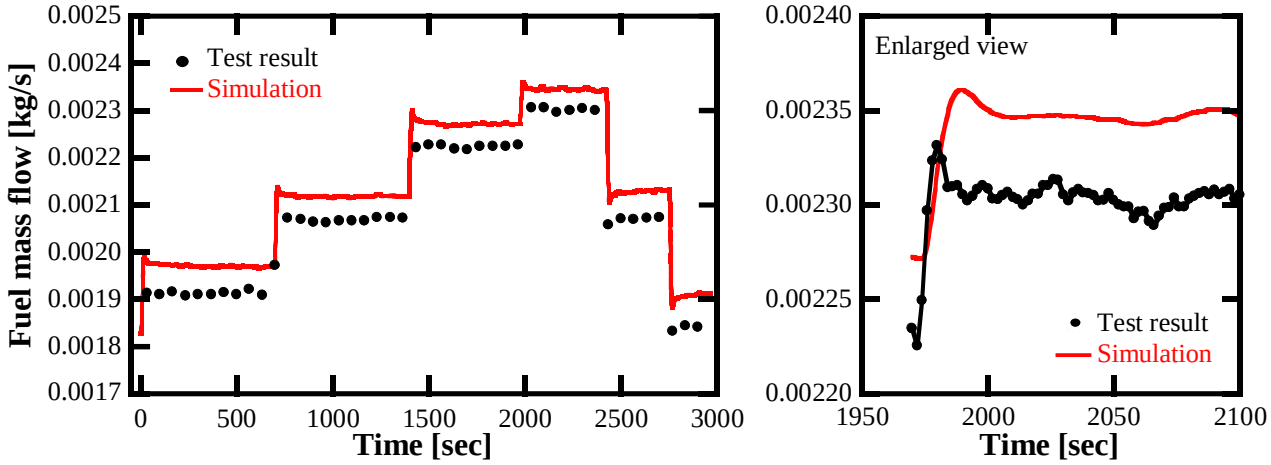

Fig. 10. Comparison of fuel flow rate between simulation and test

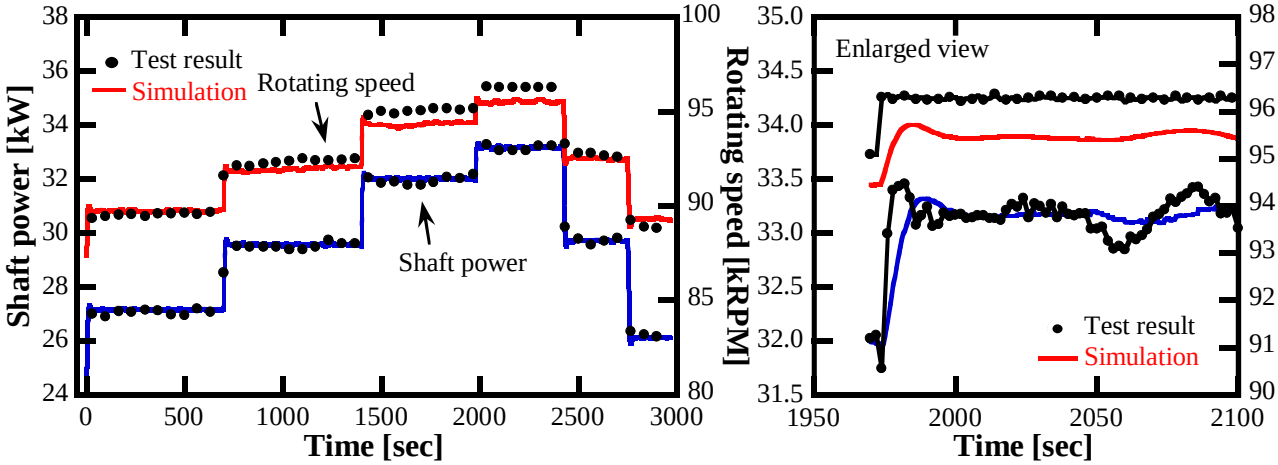

Fig. 11. Comparison of rotating speed and shaft power between simulation and test

noticed that the turbine exit temperature is very well controlled in the simulation. In the instant when a step power change is demanded, turbine exit temperature exhibits a sudden over- or under-shoot and the simulation captured the actual phenomena very well (see Fig. 12(b)). However, exhaust gas temperature changes smoothly because the thermal capacity of the recuperator provides a large thermal damping between turbine exit and exhaust. The good match of slopes of EGT changes in simulation and test is an example of the validity of the dynamic modeling of this study, especially the feasibility of the estimated thermal capacity value of the recuperator. In general, the PD control simulated the practical dynamic control successfully. A minor difference between simulation and real operation is the rate of parameter variation at the moment of a sudden power demand. All parameters change more quickly (slopes of curves are steeper) in the real operation as observed in the enlarged views. This quick response also resulted in a shorter settling time in the real operation. The main cause of this issue seems to be the sensitivity of fuel control. A quicker fuel control leads to a larger (i.e. quicker) power change, which in turn makes the imbalance between power and load larger, leading to a quicker shaft speed change. Overall, this is almost a pure control issue which can be resolved by improving the current control logic or adopting an advanced logic in the future.

4. Conclusion

This paper presented the setup procedure of a dynamic simulation program for a micro gas turbine and an application to a commercial engine. The major findings and conclusion are summarized as follows.

1. Scaled performance maps of compressor and turbine and a multi-segment heat exchanger model of the recuperator were used and a model refinement procedure using steady-state operation data

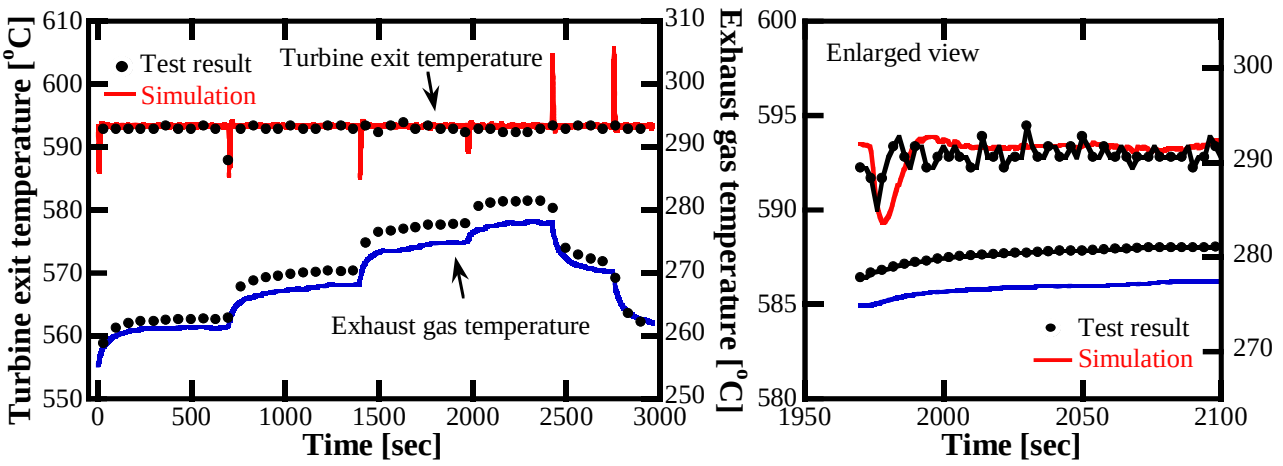

Fig. 12. Comparison of turbine exit temperature and exhaust gas temperature between simulation and test

was set up. With such a process, the lack of information on the operating characteristics of components of a commercial engine was overcome considerably.

2. The linearized calculation model of the recuperator provided a high accuracy in heat balance and a much shorter computing time compared to a non-linear model. The estimated heat transfer index was close to those in literature and remained nearly constant in a wide operation range. The agreements of simulated and measured parameters were satisfactory in a power range from a half to full load.

3. A unique method to estimate the thermal capacity of the recuperator was suggested. Comparison of the simulated variation in exhaust gas temperature during a normal shut-down process with real operating data provided the best fitting value of the thermal capacity. A smooth matching of exhaust gas temperature between simulation and real operation in a dynamic load following operation validated the feasibility of the estimated thermal capacity value.

4. Stepwise power increases and decreases with a simultaneous control target of a constant turbine exit temperature were simulated using a PD control. The real operation was reproduced very well by the dynamic simulation. In particular, turbine exit temperature which is one of the control variables was controlled with a high accuracy. A slightly slower response of the simulation compared to the real operation in the rapid power change instant was observed but this issue is expected to be resolved by an improvement in the control logic.

5. Overall, the element dynamic modeling and the suggested procedures to determine unknown critical parameter values were found to be sound. It is expected that the present program and analysis routine would provide a reliable backbone to further advances for use in engine development.

Acknowledgments

This work was supported by the Korea Institute of Industrial Technology Evaluating and Planning (KETEP) funded by the Ministry of Knowledge Economy of KOREA (MKE). (NO. 20142010102780)

Nomenclature

A	heat transfer area, m^2
c	specific heat of recuperator metal, kJ/(kgK)
c_p	constant pressure specific heat, kJ/(kgK)
CDP	compressor discharge pressure, kPa
cv	control variable

e	error
EGT	exhaust gas temperature, ºC
h	enthalpy, kJ/kg
HX	heat exchanger
I	rotating inertia, kg·m^2
i	heat transfer index
K_D	derivative gain
K_P	proportional gas
L	load, kW
M	semi-dimensionless mass flow rate, msK$^{0.5}$
m	mass, kg
$\dot{m}$	mass flow rate, kg/s
MGT	micro gas turbine
mv	manipulated variable
N	rotating speed, RPM
n	number of heat exchanger segments
P	pressure, kPa
PR	pressure ratio
T	temperature, ºC
t	time, sec
TET	turbine exit temperature, ºC
$\dot{W}$	power, kW

Greek symbols

α	convective heat transfer coefficient, kW/(m^{2}K)
η	efficiency
ω	rotating speed, rad/s

Subscripts and superscripts

C	compressor
c	cold side
D	derivative
d	design point
f	fuel
h	hot side
HX	recuperator metal
in	inlet
l	heat exchanger segment index
m	original map
me	mechanical
out	outlet
P	proportional
s	scaled map
T	turbine
t	time index

References

[1] J. H. Kim., T. W. Song., T. S. Kim., S. T. Ro., Model development and simulation of transient behavior of heavy duty gas turbines. J ENG GAS TURB POWER 2001;123:589-94.

[2] J. H. Kim., T. W. Song., T. S. Kim., S. T. Ro., Dynamic simulation of full startup procedure of heavy-duty gas turbines. J ENG GAS TURB POWER 2002;124:510-16.

[3] S. M. Camporeale., B. Fortunato., M. Mastrovito., A modular code for real time dynamic simulation of gas turbines in simulink. J ENG GAS TURB POWER 2006;128:506-17

[4] H. Asgari., M. Venturini., X. Chen., R. Sainudiin., Modeling and simulation of the transient behavior of an industial power plant gas turbine. J ENG GAS TURB POWER 2014;136:061601-1-10

[5] A. Traverso., F. Calzolari., A. Massardo., Transient analysis of and control system for advanced cycles based on micro gas turbine technology. Proceedings of ASME turbo expo 2003; 2003 June 16-19

[6] F. Ghigliazza., A. Traverso., M. Pascenti., A. F. Massardo., Micro gas turbine real-time modeling test rig verification. Proceedings of ASME turbo expo 2009; 2009 June 8-12

[7] S. Y. Kim., J. Y. Park., V. L. Goldenberg., Investigation of transient performance of an auxiliary power unit microturbine engine. Proceedings of ASME turbo expo 2006;2006 May 8-11

[8] MathWorks, MATLAB R2012b.2012

[9] R. E. Sonntag., G. J. Van Wylen., Introduction to thermodynamics. 3rd ed., US: John Wiley & Sons.1991.p.729-30

[10] Saravananmuttoo HIH., Rogers GFC., Cohen H., Gas turbine theory. 5th ed., UK: Prentice Hall.2001.p.275-76

[11] Capstone Turbine Corporation., Final technical report. DOE Project ID # DE-FC26-00CH11058.2008

[12] Capstone Turbine Corporation., Technical reference. Capstone model C30 performance. 410004-001 Rev C.

[13] Enter Software, GasTurb12. 2012

[14] J. F. Sellers., C. J. Daniele., DYNGEN - A program for calculating steady-state and transient performance of turbojet and turbofan engines. NASA TN D-7901.1975

[15] W. M. Kays., M. E. Crawford., Convective heat and mass transfer. 3rd ed., US: McGraw-Hill.1993.p.443-46

[16] D. Junqi., C. Jiangping., C. Zhijiu., Z. Yimin., Z. Wenfeng., Heat transfer and pressure drop correlations for the wavy fin and flat tube heat exchangers. APPL THERM ENG 2007;27:2066-73

[17] J. H. Kim., T. S. Kim., S. T. Ro., Analysis of the dynamic behaviour of regenerative gas turbines. P I MECH ENG A-J POW 2001;215:339-46

[18] T. S. Kim., S. H. Hwang., Part load performance analysis of recuperated gas turbines considering engine configuration and operation strategy. Energy 2006;31:260-77

[19] W. Y. Svrcek., D. P. Mahoney., B. R. Young., A real-time approach to process control. 3rd ed., US: John Wiley & Sons.2014. p. 108

[20] W. M. Kays., A. L. London., Compact heat exchangers. 3rd ed., US: KRIEGER.1993.p.204

[21] C. F. McDonald., Recuperator considerations for future higher efficiency micro gas turbines. APPL THERM ENG 2003;23:1463-87